A Review of Systems and Methodologies for the Fossil Fuel Removal Process

Pavle Boškoski, Boštjan Dolenc
Jožef Stefan Institute
Department of Systems and Control Ljubljana
Slovenia
pavle.boskoski@ijs.si

ABSTRACT: *Fossil fuel removal is an impediment in the current world for which we have many systems and methodologies. Hydrogen-dependent technologies have the potential to do this task. In the applications, there are many issues even if it has potential in applications. We focused the solid-oxide fuel cells as they offer better efficiency and return for electric conversion. During operations, thermal stress and material degradation affect durability. We review the techniques, systems, and new achievements in diagnosis and overall health management.*

Keywords: Fuel Cells, Hydrogen, Health Management

Received: 10 November 2022, Revised 2 February 2023, Accepted 16 February 2023

DOI: 10.6025/jdp/2023/13/2/38-50

1. Introduction

Energy security is one of the main pillars of our modern society. The projections for the EU energy consumptions foresee a slight decrease in our energy demand, however oil will retain its top position in the energy share of the continent. This is predominantly due to the requirements of the transportation sector. Since European oil reserves (excluding Russia) are virtually non existent it is of great importance to reduce our dependance on oil due to two main factors. First there is the obvious ecological viewpoint that supports Europe's strong dedication towards significant reduction in greenhouse gas emission. Second is from a purely financial standpoint, since oil imports amount to 15% of the overall imports by the EU. By analysing the EU energy consumption by sectors the three most energy demanding segments are transportation, residential consumers and district heating systems. Addressing the demands of these segments can significantly decrease our dependence on imported energy.

Currently we are witnessing a substantial growth in the installed renewable energy sources predominantly wind farms and solar power plants. The biggest deficiency of these systems is the intermittent nature of power generation. Therefore in

order to exploit these power sources in full while in the same time to satisfy our demand of energy it is required to provide means of efficient energy storage and energy distribution systems.

The distribution gird for electrical energy is very efficient. It estimated losses are in the range of 5% to 8% [1]. As a result, a lot of effort is put into the development of energy storage devices that can harness the electrical energy. When analysing the available technologies, the usual metrics involve two properties: energy density (Wh/kg) and power density (W/kg). On one side of the scale are batteries and fuel cells, which have high energy density but low power density. On the other side are super capacitors with somewhat lower energy density but quite high-power density. Our focus is on how energy density devices i.e. batteries and fuel cells.

Currently the leading technology in batteries development is based on Lithium. From a geo-political viewpoint, Europe is in the same situation as it is with oil. The world's largest deposits of this element are in South America and China. Therefore, in long term building our society solely on Lithium based batteries will make us highly dependent on resources that are outside of our borders.

Unlike batteries that are energy storage devices, fuel cells are energy conversion devices. They convert chemical energy stored in the hydrogen fuel into electrical energy through electrochemical combination of hydrogen and oxygen. Based on the hydrogen source, principle of operation and operating temperature, fuel cell technology distinguishes among SOFCs [2], low-temperature proton exchange membrane fuel cells (PEMFCs) [3], high temperature polymer electrolyte membranes (HT-PEMs) [4], direct methanol fuel cell (DMFC), sulphuric acid fuel cell (SAFC), molten carbonate fuel cell (MCFC), solid polymer fuel cell (SPFC), and alkaline fuel cell (AFC) [5]. Regarding fuel cells there are roughly three technology groups: low temperature PEM cells, high temperature MCFC and the so-called SOFC. Unlike batteries, that are capable of storing of electrical energy, fuel cells use hydrogen as a fuel. Consequently, when analysing the viability of fuel cell technology (or commonly referred to as hydrogen technology) vs. batteries there are several points that on first glance make the fuel cells as wrong choice. Key among them being production, compression and distribution of hydrogen. However, making a more detailed analysis provide a completely different story.

The SOFC technology offers very high conversion efficiency that is close to 60%. Therefore, using renewable energy sources in the time intervals when there is an excess of energy it is possible to produce a so called green hydrogen with very little losses.

The second issue, compression, is usually addressed from the viewpoint of mechanical compression devices that are highly inefficient in particular for low density hydrogen. However, there are currently solutions that are based on the concepts of electrochemical compression capable of reaching 1000 bars of pressure without any moving components. Consequently, the compression process can be performed with efficiency of almost 80%.

The final issue is the transportation. Compared to other parts of the world, the EU has vast and extremely well developed gas pipeline system that is currently used for delivery of natural gas to almost every household on the continent. There are already examples where hydrogen is used as a supplement to the existing natural gas. The ultimate goal is to use segments of the pipeline as a delivery system for hydrogen to the end users.

This analysis shows that hydrogen-based technologies are viable solution to the issues regarding the energy security. Even more, the SOFC technology can be built without any rare earth minerals thus completely rendering our dependence on foreign materials. In the remaining of the paper, we will present the current state of development of the SOFC based fuel cells, open issues regarding their exploitation and future trends.

2. SOFC in a Nutshell

Fuel cells consist of three adjacent layers: (i.) anode, (ii.) cathode, and (iii.) electrolyte. Figure 1 displays the basic principles and essential components of a single SOFC. The main purpose of the electrolyte is to transport oxygen ions O^{2-} from the cathode to the anode, while at the same time preventing direct contact between anode and cathode chambers. The ions are formed via oxygen reduction reaction at the cathode, which is continuously fed with oxygen. On the other side, at the anode, the O^{2-} ions react with hydrogen in the process of hydrogen oxidation. In addition to H_2O, two electrons and some heats are released. The electrons travel through the external load to reach the cathode, where they participate in oxygen reduction reaction. In addition,

one of the major advantages of the SOFC is its ability of internal reforming of the fuel. This property allows the fuel cells to operate not only on pure hydrogen, but on also other hydrogen rich fuels, such as methane.

Theoretically, the voltage of a single SOFC can reach up to 1.2 V, depending on temperature, pressure and gas composition. The power output, however, is heavily conditioned with the active area of the fuel cell. Typically, the larger the active area of the cells, the higher the power output. However, the limiting factor for the size of the individual fuel cells is related to the thermo-mechanical stress induced due to thermal expansion coefficient (TEC) mismatch of the adjacent layers. With larger cells, temperature gradients over the cells become larger, thus causing higher stress on the materials, hence compromising their safe operation. Therefore, to increase power output, a number of fuel cells is connected in parallel to form a fuel cell stack.

Since the SOFCs operate at high temperatures, the stack is usually enclosed in an insulated housing to reduce heat losses. The stack then connects with a balance of plant (BOP) module, which carries out the pre-treatment of the incoming gases. Depending on the scale of the installation, the BOP consists of different interconnected components, such as heat-exchangers, blowers, fuel reformers, pipes, valves, etc.

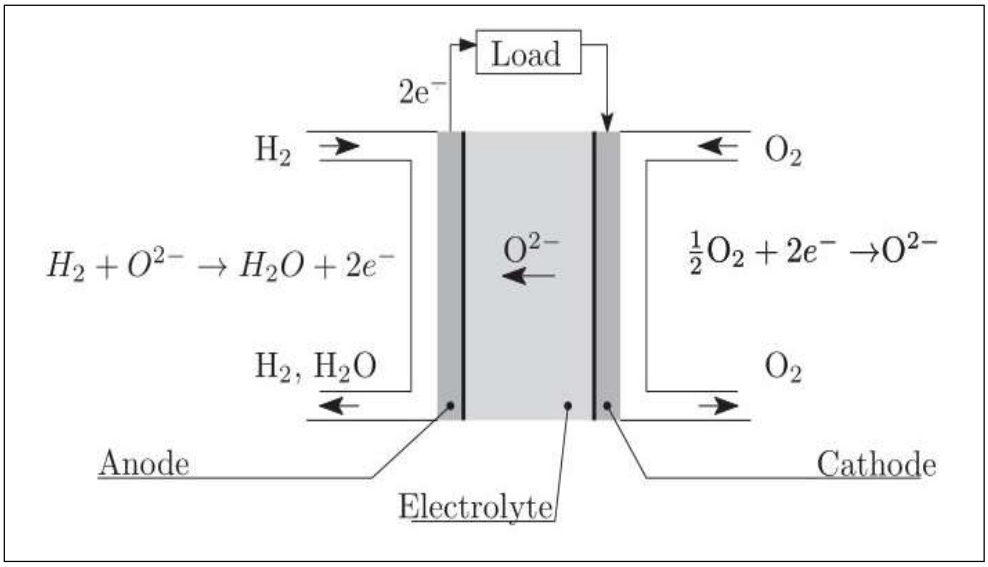

Figure 1. The basic principles of a SOFC and its essential components

3. PHM in Fuel Cells

The degradation occurring within the fuel cells inherently impedes the efficiency of power conversion. Apart from the fact a great deal of effort has been dedicated to the understanding of SOFC degradation mechanisms [6], only a relatively limited set of diagnostic approaches is available.

The PHM can be defined as a set of activities in which the main perspective is to enhance the effective reliability and availability of a product in its life-cycle conditions by detection of current and approaching failures [7].

Figure 2 shows basic self-contained building blocks of an PHM system, divided in seven layers. On the lower levels L1 the data is collected employing sensors and transducers. In the data processing level, features that carry information about the condition of an underlying system are extracted from the collected data. Further up, in the condition assessment layer, the features are evaluated in a sense that any deviation from 3 Ohrid, North Macedonia, 27-29 June 2019 the normal operation is detected. If changes in the behaviour are detected, then the fault alarms are triggered. In the next stage, in the diagnostic layer, the patter of the triggered alarms are compared with known failure modes to possibly identify the cause of the triggered alarms. Having identified the faulty component, the prognostics layer aims to predict how the component in question will operate in future based on the historic data from the previous layers.

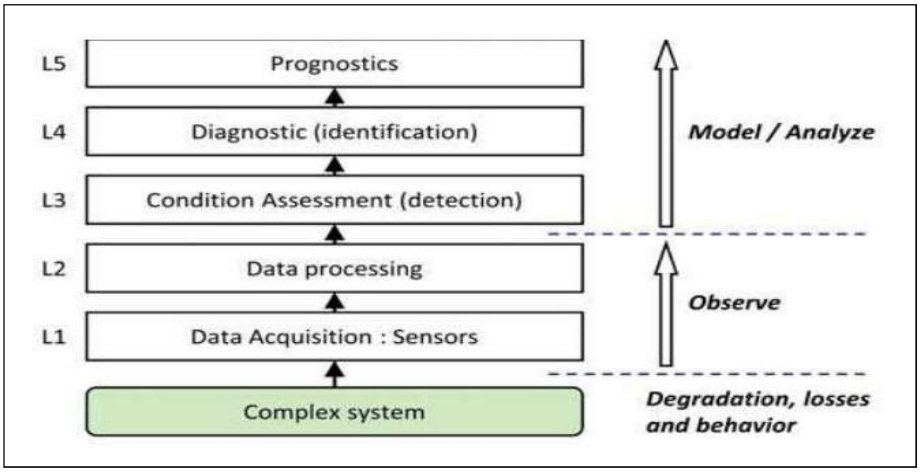

Figure 2. PHM structure from [8]

Within this framework, several passive fault detection and identification (FDI) approaches have been proposed to constantly monitor components that supply and pre-treat fuel before entering the reaction chambers of the fuel cells. That encompasses several analytical model-based approaches [9], [10], black-box approaches [11] and signal processing approaches [12]. However, yet the most predominate approaches to health assessment build on the use of electrochemical impedance spectroscopy (EIS). Characteristic for EIS is that applies local probing directly on the fuel cells in order to excite all the relevant dynamic modes related to chemical processes in the system to gain more detailed information about condition of the cells themselves. Although it has been around for several decades, the way it is used has not changed much.

Conventional EIS techniques use low-amplitude sinusoidal excitation, repeatedly performed at different frequencies, from which then the gain and phase of the points on the Nyquist curve are estimated. Such an approach suffers from too long probing time that is usually required to obtain high-quality EIS spectra. That means too long perturbation of the process in operating mode. Particularly critical is estimation of EIS curve at low frequencies as normally several periods of a sinusoid are required to extract precise information.

By applying excitation over a wide range of frequencies simultaneously, the authors in [13] showed that the same quality of the results as in conventional EIS can be obtained at the substantially shorter probing times (an order of magnitude). The evaluation of EIS curve is done by post-processing of the current and voltage signals by means of complex wavelet transform. Apart of the much shorter probing session, additional benefit is also much better resolution of the EIS curve obtained compared to the conventional EIS, as it is defined by the sampling rate. Savings in required probing times can gradually diminish when the required precision of the spectral reconstruction at low frequencies is increasing.

The measured EIS data can then be further processed to extract relevant information about the health status. Here, several approaches serve as tools the EIS data have to be interpreted either through the change of the pattern of the EIS curve, or by interpreting changes in the parameters of the equivalent circuit models (ECM) [14], [15] and distribution of relaxation times (DRTs) [16].

3.1. Data Acquisition

A block scheme of the data acquisition system consisting of several interconnected components is shown in Figure 3. It includes programmable digital load, data acquisition device, a current probe, and controlling unit that connects the functionality of all the components.

An electronic load is connected directly in series with the SOFC and is used to set DC current as well as to superimpose various excitation signals. This way, the current in the system is controlled by the load, and defined by the system operator. In more industrial circumstances, the electronic load can be also replaced by incorporating its functionality in power conditioning unit which is then connected to the electric grid. However, by doing so, one needs to keep in mind the limitations of connected power electronics when designing the excitation signals. The electrical current is measured using a non-invasive

current probe which offers sufficiently high bandwidth and does not disturb the functionality of the system. The data acquisition hardware allows for individual cell voltages and the output of the current probe to be measured simultaneously. This way individual cells can be monitored at the same time and allow for more accurate isolation of the possibly faulty cell. Figure 4 show an excerpt from the data collected during one probing.

The electronic load and the data acquisition hardware are connected to a computer that orchestrates the probing. First the electronic load is triggered to superimpose the excitation signals to the system while the the response from the cells and current probe are logged. Furthermore, the computer allows to design a schedule of experimental probing to facilitate automated and regular experiments. If needed the computer can also be used to process the data on sight, or send it to the cloud.

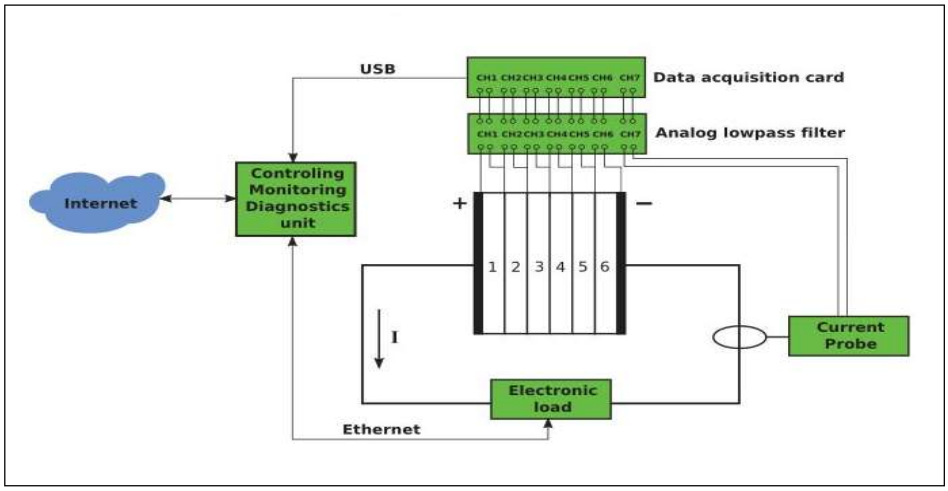

Figure 3. Block scheme of the system for impedance characterisation of electrochemical energy devices

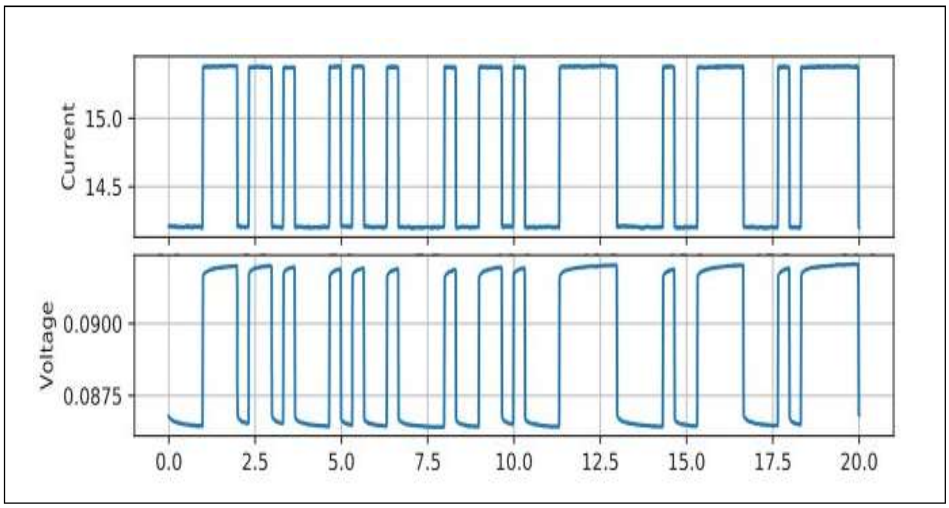

Figure 4. An example of the data collected on a single SOFC

3.2. Data Processing and Feature Extraction

The conventional frequency domain signal analysis performed with the Fourier transform, provides a detailed picture of the frequency components present in the signal but without any information regarding their time occurrence and duration. Time-frequency analysis offers a solution to this problem thus providing the information about the temporal details as well. Typical examples are the Short-time Fourier transform, Wigner-Ville distribution, wavelet transform etc.

Regardless of the selected method there is a theoretical limitation on the joined time-frequency resolution. Unlike other methods, the wavelet transform enables flexible selection of the desired time-frequency resolution by introducing the concepts of scaling. Wavelet transform is based on a set of specifically designed functions called wavelets. The continuous wavelet transform (CWT) of a square integrable function $f(t)$ is defined [17]

$$Wf(s,u) = \int_{-\infty}^{\infty} f(t)\, \Psi^*_{u,s}(t)dt \tag{1}$$

where wavelet function $\Psi^*_{u,s}(t)$ is scaled by s and translated by u version of original mother wavelet $\Psi(t)$:

$$\Psi^*_{u,s}(t) = \frac{1}{s}\Psi\left(\frac{t-u}{s}\right) \tag{2}$$

The key parameter in CWT is the selection of the wavelet function. EIS analysis requires information about the amplitude and phase of the excitation and response signals, the rover a complex Morlet wavelet function is readily available [18]: The time and frequency localisation is determined through the parameters u and s respectively. More details regarding the properties of the Morlet wavelet and the application of CWT for EIS analysis can be found in [13].

The voltage/current signal pairs from Figure 4 are transformed employing (1), divided and averaged over time to obtain Nyquist curve show in Figure 5.

1) Feature extraction: Observing changes in Nyquist curves can be directly employed for detecting a change in a system and condition monitoring. However, a more concise information is required to facilitate the identification of degradation mechanism. This can be achieved by modeling the measured Nyquist curve in one way or another and is often referred to as deconvolution of the EIS spectra.

Generally speaking, there are two approaches to deconvolution of the EIS spectra: (i.) ECM modeling through non-linear optimisation (ii.) non-parametric identification of the Nyquist curve through DRT [19]. From mathematical point of view the above approaches are equivalent. That is, having one of the two, one can easily derive the other one [20].

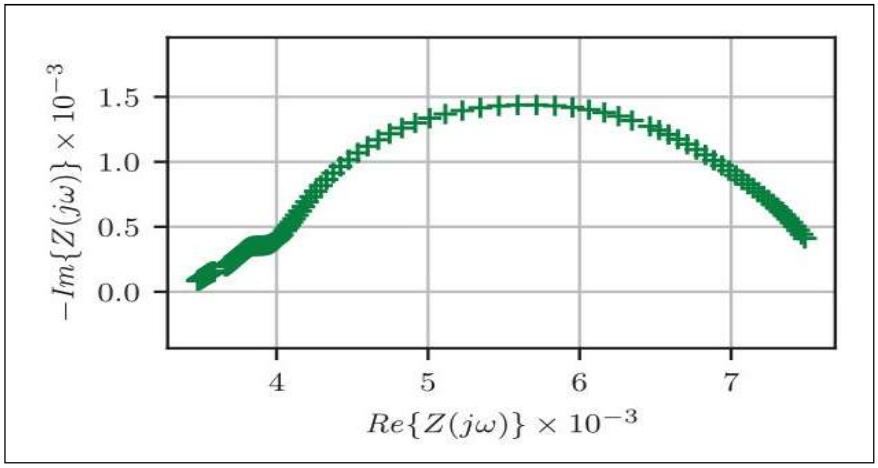

Figure 5. An example of a Nyquist curve of a single SOFC

An ECM of fuel cell impedance can be described as a series of RQ elements connected in series, as shown in Figure 6. It has been shown that the degradation phenomena manifest in the changes of the parameters of the ECM. Indirect observations through DRT have recently been published [21]. Therefore, the parameters of the ECM can be employed to identify ongoing degradation mechanism.

There are several ways to estimate the parameters of any model. For instance, having a fuel cell impedance model structure

$$Z(j\omega) = R_s + \sum \frac{R_i}{\tau_i (j\omega)^{\alpha_i} + 1} \tag{3}$$

one can formulate an optimisation problem

$$\underset{\theta}{argmin}\, c(\theta)$$

where $c(\theta)$ denotes a loss function which describes *goodness of fit* of the model with respect to measured Nyquist curve, and the θ is a vector of model parameters. Following this approach one obtains a point estimate of parameter values.

In order to obtain richer insight regarding the accuracy of the estimates statistical based approaches can be employed. The main is as follows. Given a model and data D, the posterior distribution of the model parameters θ can be estimated via Bayes rule as:

$$P(\theta \mid D) = \frac{P(D \mid \theta)\ P(\theta)}{\int P(D \mid \theta)\ P(\theta)\, d\theta} \tag{4}$$

where $p(D|\theta)$ is *likelihood*, $p(\theta)$ is *prior*, and $\int p(D|\theta)\, p(\theta)\, d\theta$ is called marginal likelihood or model *evidence*.

By constructing likelihood function and defining prior probabilities (typically uninformative ones), the posterior of the model parameters can be inferred employing four different approached: (i.) analytically in the case of the tractable required mathematical operations, (ii.) employing numerical integration techniques (iii.) through Markov chain Monte Carlo (MCMC) simulations, (iv.) employing variational Bayes approximation.

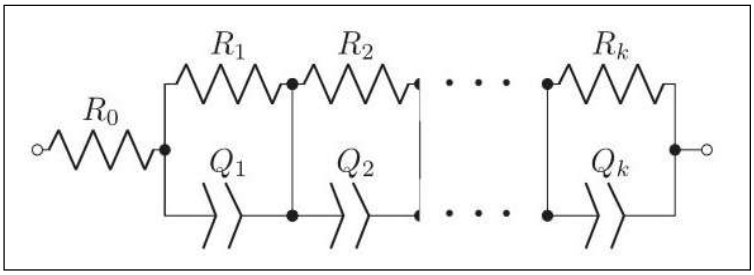

Figure 6. General form of the ECM using RQ-elements

More on MCMC methods, and Bayesian inference, can be found in [22].

In this case a sequence of three *RQ* elements, $i \in \{1, 2, 3\}$, the posterior distributions of the model parameters are shown in Figure 7. In particular, for each of the three *RQ* elements $i \in \{1 \ldots 3\}$, top row shows time constants τ_i, second row shows resistances R_i, and third row shows their corresponding α_i exponents. The bottom row shows serial resistance. Note that the parameters that belong to individual *RQ* element are denoted with the same colour.

3.3. Fault Diagnosis

The onset of faults typically results into a change of the extracted feature values. The problem of reliable change detection in selected feature is outlined in Figure 8. The righthand figure shows the desired scenario i.e. the feature values exhibit steady growth. Once the value surpasses the predefined threshold an alarm is triggered. However, in the case of incipient faults, the extracted feature values become close to a pre-determined threshold value. Due to small variations one can observe numerous short periods when the feature value is higher than the threshold. This may lead to excessive rate of false alarms, and thus

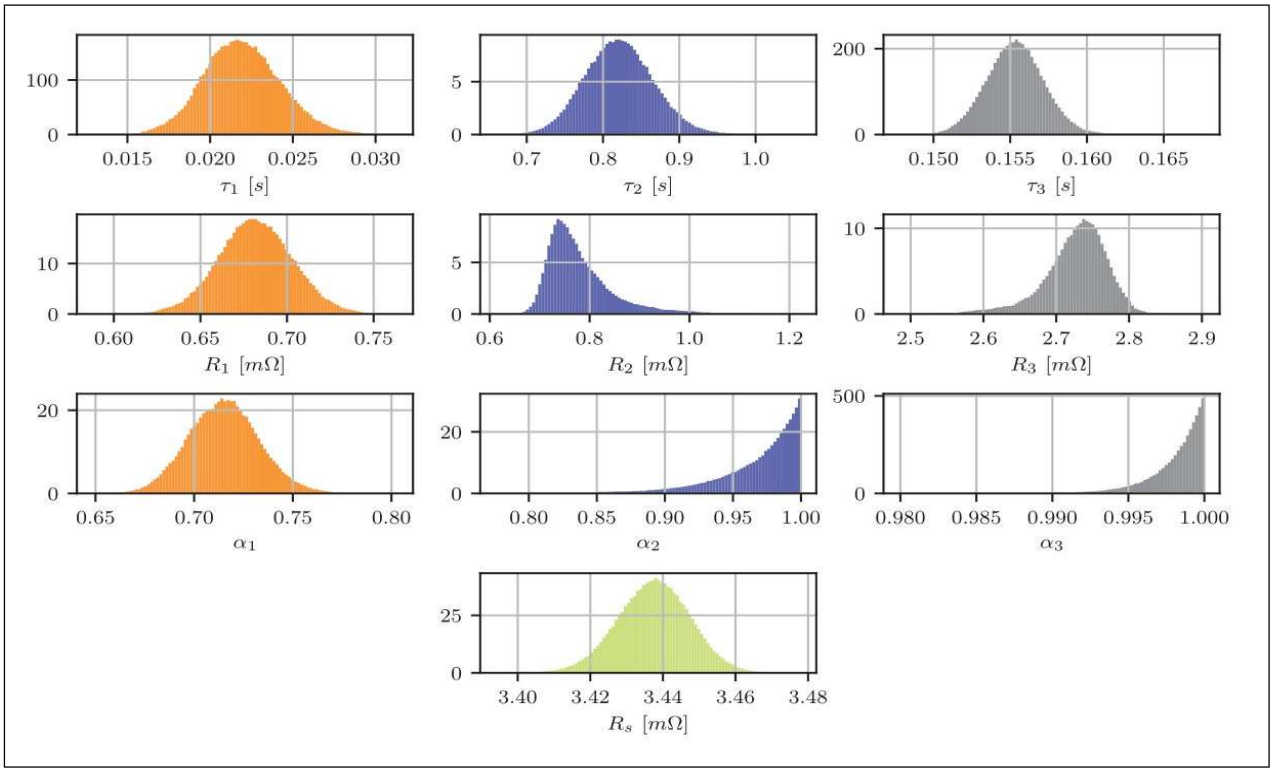

Figure 7. Posterior probability density functions (PDFs) of the model parameters.

reducing the confidence in the PHM system as a whole. This is a known problem that is usually solved either by employing some sort of filtering approaches or increasing the threshold values. Filtering approaches reduce the response time of the detection system, whereas increasing the threshold values reduces the its sensitivity. These problems can be resolved by employing robust statistical tests.

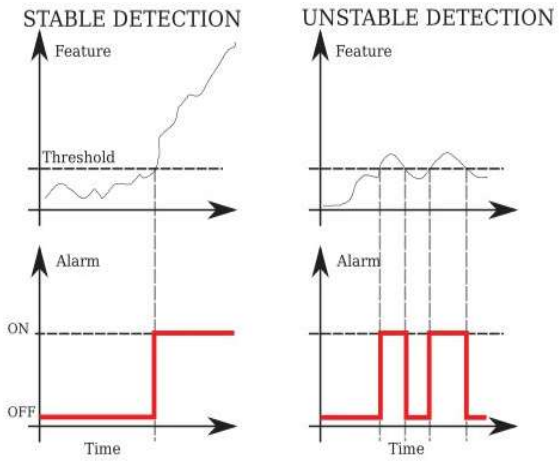

Figure 8. Problem with detection detection stability

A change is established by quantifying dissimilarity among the features' statistics in current and nominal fault-free state. 6 Ohrid, North Macedonia, 27-29 June 2019 by calculating Jensen-Rényi (JR) divergence among empirical distributions of the features, the need for known operating conditions and data records at various system failures is avoided. The approach was initially developed for vibration-based diagnostics for gears and bearings under constant and variable operating conditions, here is adopted for change detection in the parameters of an ECM, such as the one presented in previous section.

To this end, the change detection algorithm builds on generalised JR divergence to quantify the dissimilarity among two or more PDFs. The JR divergence JR_{α}^{w} quantifies dissimilarity among n PDFs:

$$JR_{\alpha}^{\omega}(P_1, \ldots, P_n) = H_{\alpha}\left(\sum_{i=1}^{n} \omega_i P_i\right) - \sum_{i=1}^{n} \omega_i H_{\alpha}(P_i), \quad (5)$$

In (5) H_{α} is Rényi entropy and $\sum_{i=1}^{n} wi = 1$. The selection of weights w_i in (5) is in principle arbitrary. With w_i selected uniformly i.e. $w_i = 1/n$, the divergence reaches maximal value.

JR divergence quantifies shared information among n random variables. If they are identical, i.e. $P_1 = P_2 = \ldots = P_n$, divergence is zero. However, if one of them deviates even slightly, the JR divergence becomes different from zero. Therefore, JR divergence carries information about dissimilarity among n PDFs.

Since we are seeking a way to detect a change in the statistics of the parameters of an ECM which were estimated in the previous section, JR divergence offers an elegant solution. To detect a change in the parameter, all that is needed is a reference set where the fuel cell was operating under normal operation. Once the reference data is available, we can compare the online estimates of the model parameters with the reference ones. This is demonstrated in Figure 9. To be more precise, Figure 9a shows how one of the parameters in from Figure 7 behaved during a 600h long durability experiment of an SOFC short stack comprising of 6 cells. During this test, the data was collected every 6 hours. The figure was obtained by processing the data as described above in the paper. Note that there are three events that were intentionally triggered, which are marked by yellow strips. It is apparent that the selected condition monitoring parameter is affected by these changes. After the first event, the cell recovered, however, after the second experiment the cell remained permanently damaged. The change detection facilitated by employing JR divergence is shown in 9b. In this case, 10 PDFs were included in a reference data set, and compared with a set of 10 in an "online" mode. The JR divergence detects a first change in the parameter clearly, thus triggering the alarm. After this first event the cell stabilised and returned to normal operation. Further in the experiment, the the second event also caused severe change in the parameter. The algorithm clearly detected this change. However, after this second event the cell never recovered to its original state, hence the value of JR divergence remained at high level.

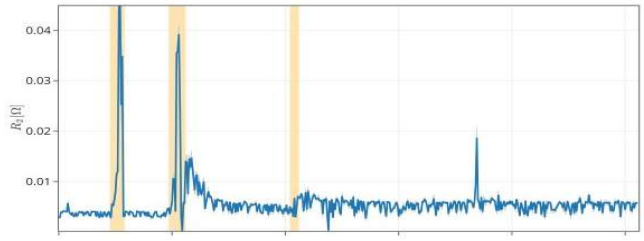

(a) Time evolution of the parameter

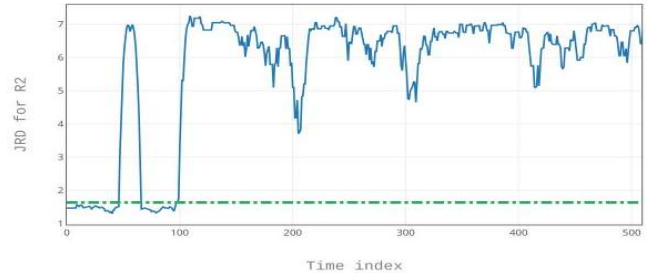

(b) JR divergence-based change detection

Figure 9. Results of the proposed JRD based fault detection approach employed on a 3000 hours SOFC run-to-failure experiment

3.4. Prognostics

Various approaches to condition monitoring have been proposed with the aim to detect the onset of fault and hence allow for the design of accommodation actions [6], [23]. However, for safety reasons and maintenance purposes, the information of particular practical value is how long will the system operate prior to its end of life (EOL). Relatively little attention has been devoted to the development of algorithms for predicting SOFC remaining useful life (RUL).

So far, some more work has been done in the area of proton exchange membrane (PEM) fuel cells. Although PEM and SOFC differ in many aspects, it is worth screening the main ideas applied to PEM. For example, in [24], the authors discussed and summarised challenges related to PEM fuel cell prognostics and RUL predictions. The authors identify the importance of suitable health indicators for RUL prediction and address the definition of EOL point of fuel cells.

Works related to RUL prognosis in PEM aim at modelling temporal evolution of stack voltage, voltage related power output, or efficiency due to degradation [24]. The most common approach is to consider voltage as state of health (SOH) indicator and perform RUL upon evident drift in stack/cell voltage. Such a characterisation of SOH is often justified because voltage is directly associated with power output, and hence the efficiency of power conversion. Relatively few works define SOH differently, see e.g. [25]. Various empirical models are then employed in order to predict voltage drop in future and estimate RUL. The employed models range from simple ones with linear, polynomial and exponential structures [26], to complex structures common in machine learning society [27]– [30].

However, from the practical point of view, such approaches become quickly unsatisfactory, especially under varying operating conditions. This issue was recently addressed and published by the authors [31]. In the aforementioned paper, the authors propose an estimator of stack's internal resistance, such as the one in Figure 7, by employing an Unscented Kalman filter (UKF).

1) RUL estimation: The main concept of RUL estimation is outlined in Figure 10. At each time moment k, when current estimates of internal resistances become available, the model parameters are updated. Next, the model is used in open-loop simulations until time step $k+N$, when the modelled feature crosses a pre-defined failure threshold. RUL is then simply N number of steps multiplied by the sampling time.

The RUL plot displayed in lower part of Figure 10 is obtained by plotting estimated RUL distribution at each time moment k. An example of such a plot is shown in Figure 11. Explanation of the Figure is as follows. The x-axis shows running time, while the y-axis displays the RUL distribution. *True* RUL is denoted by dashed thick line and it shortens linearly in time. The blue thick line is the estimate most probable value of RUL, while the coloured contours plot corresponding distribution. In the beginning of the experiment, when only a little information about the degradation is available, the predictions are poor. With time passing, the stack degrades further and the model incorporates this new information. Thus, model becomes more accurate and is able to predict RUL more accurately. More details can be found in [31].

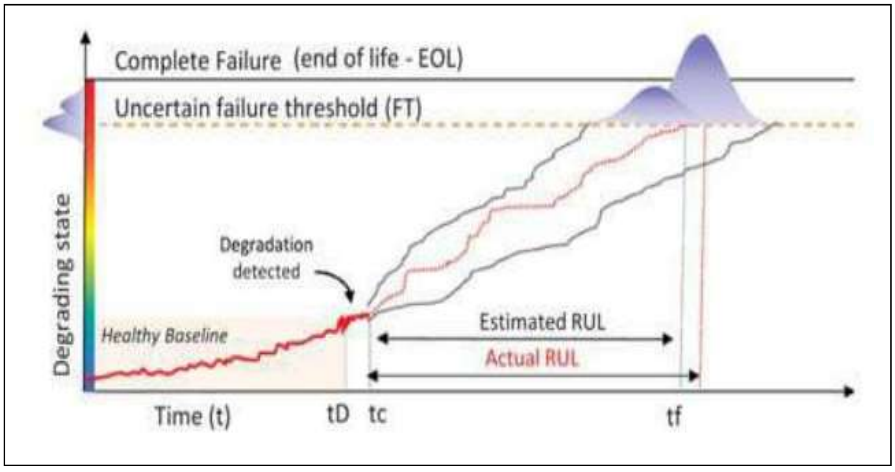

Figure 10. RUL prediction concept

2) Degradation Modelling: In order to be able to perform accurate RUL estimation accurate degradation models are required. Although, degradation is a very complicated process, sufficiently accurate RUL estimations can be achieved using quite simple approaches.

One of such models described in [32] reads:

$$r_d(F,T,j) = \frac{0.59\mathrm{FU} + 0.74}{1 + e^{\left(\frac{\mathrm{T}-1087}{22.92}\right)}} \left(e^{2.64\mathrm{j}} - 1\right). \quad (6)$$

where r_d is the degradation rate, *FU, T* and *j* are fuel utilisation, temperature, and current density, respectively. These are all process variables, which can be manipulated and controlled in order to minimise the degradation rate. Model (6) was recently adopted for predicting how the fuel cell stack will degrade in future [33]. The parameters, i.e. numeric values in (6) were estimated from the data employing Bayesian approach.

The prediction results are shown in Figure 11. The results show that 800 hours before the end-of-life, the model accurately predicts the RUL. Furthermore, the variance (uncertainty) of the predictions are decreasing as the time progresses i.e. the model predictions are becoming more precise as we approach the end-of-life.

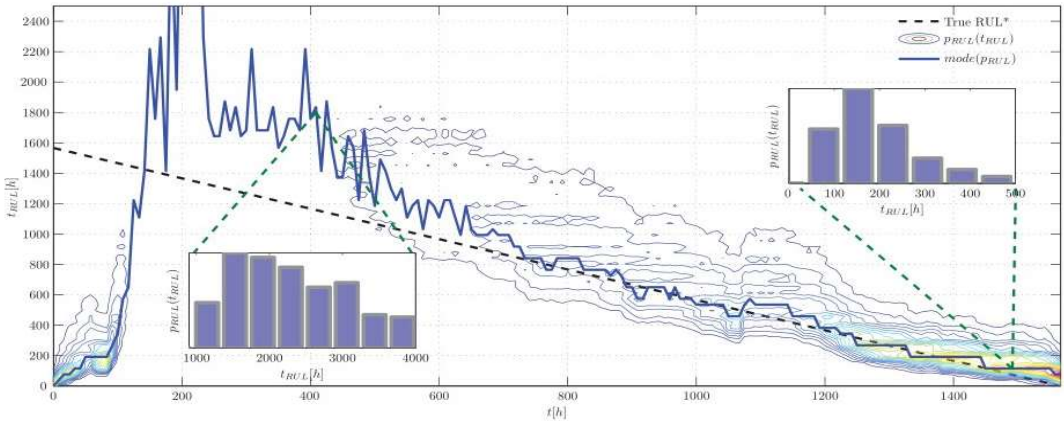

Figure 11. RUL predictions for the entire duration of the experiment. The contour plot contains three elements: (i.) experimental RUL, (ii.) RUL distribution for each time moment *k* with support *tRUL*, and (iii.) mode of the corresponding RUL distribution marking the most probable *tRUL*

4. Conclusion

The presented results addressed three aspects of PHM for SOFCs. A solution is provided regarding the feature extraction using fractional order models of SOFCs. Based on the statistical properties of these features a reliable change detection algorithm is proposed. The algorithm is based on multi-dimensional JR divergence. Finally, a computationally efficient algorithm for RUL estimation is presented.

Taking into account the maturity level of the SOFC technology, we should be witnessing an increased number of installations of such systems. By doing so we will become more self-reliable in the context of energy security, since all the raw materials required for these systems are readily available in our region. Furthermore, the fuel cell technology, in particular SOFC, provides an approach for local fuel production. All these benefits makes the hydrogen technology a viable candidate in the process of seeking alternative to our dependence of fosill fuels.

Acknowledgements

The authors would like to acknowledge the support of the Slovenian Research Agency through the research programme P2-0001.

References

[1] Energy, Transport and Ghg Emissions Trends to 2050.

[2] Singhal, S.C. and Kendall, K. (2003). High Temperature Solid Oxide Fuel Cells: Fundamentals, Design, and Applications. Elsevier: Amsterdam.

[3] Barbir, F. (2013) PEM fuel cells. *Theory into Practice.* Elsevier: Amsterdam.

[4] Li, Q., Aili, D. and Jensen, H., editors (2016). *High Temperature Polymer Electrolyte Membrane Fuel Cells*. Springer: Berlin.

[5] Kirubakaran, A., Jain, S. and Nema, R.K. (2009) A review on fuel cell technologies and power electronic interface. *Renewable and Sustainable Energy Reviews*, 13, 2430–2440.

[6] Barelli, L., Barluzzi, E. and Bidini, G. (2013) Diagnosis methodology and technique for solid oxide fuel cells: *A review. International Journal of Hydrogen Energy*, 38, 5060–5074.

[7] Jouin, M., Gouriveau, R., Hissel, D., Péra, M.-C. and Zerhouni, N. (2013) [Online]. Available: www.sciencedirect.com/science/article/pii/S036031991302274X Prognostics and health management of pemfc – State of the art and remaining challenges. *International Journal of Hydrogen Energy,* 38, 15307–15317.

[8] Lebold, M. and Thurston, M. (2001) Open standards for condition-based maintenance and prognostic systems 5th Annual Maintenance and Reliability Conference.

[9] Marra, D., Pianese, C., Polverino, P. and Sorrentino, M. (2016). Models for Solid Oxide Fuel Cell Systems*: Exploitation of Models Hierarchy for Industrial Design of Control and Diagnosis Strategies*. Springer: Berlin.

[10] Sorce, A., Greco, A., Magistri, L. & Costamagna, P. (2014) FDI oriented modeling of an experimental SOFC system, model validation and simulation of faulty states. *Applied Energy*, 136, 894–908.

[11] Sorrentino, M., Marra, D., Pianese, C., Guida, M., Postiglione, F., Wang, K. and Pohjoranta, A. (2014, ati 2013) On the use of neural networks and statistical tools for nonlinear modeling and on-field diagnosis of solid oxide fuel cell stacks. *Energy Procedia,* 45, 298–307- 68th Conference of the Italian Thermal Machines Engineering Association.

[12] Pahon, E., Yousfi Steiner, N.Y., Jemei, S., Hissel, D., Péra, M.C., Wang, K. and Moçoteguy, P. (2016) Solid oxide fuel cell fault diagnosis and ageing estimation based on wavelet transform approach. *International Journal of Hydrogen Energy,* 41, 13678–13687.

[13] Boškoski, P., Debenjak, A. and Mileva, B. (2017) Boshkoska, Fast Electrochemical Impedance Spectroscopy as a Statistical Condition Monitoring Tool, ser. *SpringerBriefs in Applied Sciences and Technology. Springer International Publishing*.

[14] Polverino, P., Sorrentino, M. and Pianese, C. (2017) A model-based diagnostic technique to enhance faults isolability in solid oxide fuel cell systems. *Applied Energy*, 204, 1198–1214.

[15] Rezaei Niya, S.M.R., Phillips, R.K. and Hoorfar, M. (2016) Process modeling of the impedance characteristics of proton exchange membrane fuel cells. *Electrochimica Acta*, 191, 594–605.

[16] Heinzmann, M., Weber, A. and Ivers-Tiffée, E. (2018) Advanced impedance study of polymer electrolyte membrane single cells by means of distribution of relaxation times. *Journal of Power Sources*, 402, 24–33.

[17] A Wavelet Tour of Signal Processing (Third Edition) (2009) (edited by M. Stéphane). Academic Press: Cambridge, USA.

[18] Iatsenko, D., McClintock, P.V.E. and Stefanovska, A. (2015) [Online]. Available: https://link.aps.org/doi/10.1103/ Nonlinear mode decomposition: A noise-robust, adaptive decomposition method. *Physical Review. E, Statistical, Nonlinear, and Soft*

Matter Physics, 92, 032916 [PubMed: 26465549]. PhysRevE.92.032916

[19] Ciucci, F. and Chen, C. (2015) [Online]. Available: www.sciencedirect.com/science/article/pii/S0013468615007203 Analysis of electrochemical impedance spectroscopy data using the distribution of relaxation times: *A bayesian and hierarchical bayesian approach. Electrochimica Acta,* 167, 439–454.

[20] Fuoss, R.M. and Kirkwood, J.G. (1941) Electrical properties of solids. viii. dipole moments in polyvinyl chloride-diphenyl systems*. *Journal of the American Chemical Society,* 63, 385–394.

[21] Caliandro, P., Diethelm, S. and Van herle, J. (2017) [Online]. Available: https://onlinelibrary.wiley.com/doi/abs/10.1002/fuce.201600196 Triode Solid Oxide Fuel Cell Operation Under Sulfur-Poisoning Conditions. *Fuel Cells*, 17, 457–463.

[22] Kruschke, J.K. (2010). Do in Bayesian Data Analysis.

[23] Polverino, P., Pianese, C., Sorrentino, M. and Marra, D. (2015) Model-based development of a fault signature matrix to improve solid oxide fuel cell systems on-site diagnosis. *Journal of Power Sources*, 280, 320–338.

[24] Jouin, M., Gouriveau, R., Hissel, D., Péra, M.-C. and Zerhouni, N. (2016) Degradations analysis and aging modeling for health assessment and prognostics of PEMFC. *Reliability Engineering and System Safety*, 148, 78–95.

[25] Zhang, X. and Pisu, P. (2012) An unscented kalman filter based approach for the health monitoring and prognostics of a polymer electrolyte membrane fuel cell. In: *Annual Conference of Prognostics and Health Management Society*.

[26] Kimotho, J.K., Meyer, T. and Sextro, W. (2014) PEM fuel cell prognostics using particle filter with model parameter adaptation. *In: IEEE Conference on Prognostics and Health Management*, pp. 1–6.

[27] Silva, R.E., Gouriveau, R., Jemeï, S., Hissel, D., Boulon, L., Agbossou, K. and Yousfi Steiner, N. (2014) Proton exchange membrane fuel cell degradation prediction based on adaptive neuro-fuzzy inference systems. International Journal of Hydrogen Energy, 39, 11128–11144, p. 11.

[28] Morando, S., Jemei, S., Gouriveau, R., Zerhouni, N. and Hissel, D. (2014) Fuel cells remaining useful lifetime forecasting using echo state network. *In: IEEE Vehicle Power and Propulsion Conference*, pp. 1–6.

[29] Javed, K., Gouriveau, R. and Zerhouni, N. (2015) Data-driven prognostics of proton exchange membrane fuel cell stack with constraint based summation-wavelet extreme learning machine. *In: 6th international conference on fundamentals and development of fuel cells*, pp. 1–8.

[30] Hochstein, A., Ahn, H., Leung, Y. and Denesuk, M. (2014) Switching vector autoregressive models with higher-order regime dynamics. *In: IEEE Conference on Prognostics and Health Management (PHM)*, no. 1-10.

[31] Dolenc, B., Boškoski, P., Stepanèiè, M., Pohjoranta, A. and Juricic, Đ. (2017) State of health estimation and remaining useful life prediction of solid oxide fuel cell stack. *Energy Conversion and Management*, 148, 993–1002.

[32] Zaccaria, V., Tucker, D. and Traverso, A. (2016) A distributed real-time model of degradation in a solid oxide fuel cell, Part i: Model characterization. *Journal of Power Sources*, 311, 175–181.

[33] Dolenc, B. (2019) Characterisation of coupling functions between process and degradation dynamics in solid oxide fuel cells. *Philosophical Transactions of the Royal Society of London Series*. Part A.